

Reconstructing a non-linear interaction in the dark sector with cosmological observations

Jiangang Kang*

*National Astronomical Observatories, Chinese Academy of Sciences, Beijing 100101, China
CAS Key Laboratory of FAST, National Astronomical Observatories,*

Chinese Academy of Sciences, Beijing 100101, China and

School of Astronomy and Space Science, University of Chinese Academy of Sciences, Beijing 100049, China

In this work we model two non-linear directly interacting scenarios in dark sector of the universe with the dimensionless parameter α and β , which dominate the energy exchange between dark energy and dark matter. The central goal of this investigation is to research the interacting model and discuss the cosmological implications based on the current observational datasets. The class of the interaction is generally characterized by a coupling function $Q \propto H(z)\rho_x$, x denotes the energy density of dark matter or dark energy. The constrained results we obtained indicate that the direct interaction in cosmic dark sector is favored by various observational data and the key effects on CMB power spectrum and linear matter power spectrum appear compared to Λ CDM standard paradigm. Finally, we discuss in depth the effect of different neutrino mass hierarchy on matter power spectrum and the variation of the ratio of CMB temperature power spectrum C_ℓ^{TT} and matter power spectrum $P(k)$ when the $\Delta N_{eff} = N - 3.046$ from 0.5 to 2, respectively.

Keywords: dark energy; dark matter; cosmological observations; cosmological parameters; neutrinos.

I. INTRODUCTION

The accelerated expansion of the late-time Universe since was discovered by observations of type Ia supernovae [1, 2], understanding the physical nature behind the acceleration is one of the fundamental topics in modern cosmology.

An exotic species of the energy with the equation of state $w_d^{eff} = P_d/\rho_d < -\frac{1}{3}$ dubbed as dark energy (DE) has been introduced [3, 4] to explain the expansion of the Universe. Based on Einstein's theory of General Relativity (GR), the dark energy is represented by the cosmological constant Λ , which combines with the pressureless cold dark matter (CDM) have regarded as a standard model for modern cosmology.

Many predictions from the standard Λ cold dark matter (Λ CDM) theory have been successfully verified by a variety of astronomical observations. However, there are still several challenging puzzles which need to be addressed, (i) the so-called fine tuning problem, i.e. the result of the vacuum energy density based on quantum theory reaches some 120 orders of magnitude larger than that inferred from the cosmological constant Λ [5, 6]; (ii) coincidence puzzle: is that the energy density of DM and DE are approximate one order of magnitude, although the two quantities do not share similar evolution laws and have different rates of evolution as the universe expands, so why do they happen to be of the same order of magnitude right now? [4, 7–12]; (iii) the Hubble constant tension: the $H_0 = 67.4 \pm 0.5 \text{ km s}^{-1} \text{ Mpc}^{-1}$ derived from Planck 2018 (P18) Cosmic Microwave Background (CMB) [13, 14] determination in Λ CDM is less than 4.4σ error than $H_0 = 74.03 \pm 1.82 \text{ km s}^{-1} \text{ Mpc}^{-1}$ obtained directly from the local distance ladder measurements of SN Ia (R19) [15]; (iv) the estimated root-mean-square mass fluctuation amplitude σ_8 in $8h^{-1} \text{ Mpc}$ spherical volume and matter energy density Ω_m from the Planck 2018 CMB measurements [13, 16] under the Λ CDM cosmology is different from that derived from weak lensing effects based on the KiDS survey [17–19]. Therefore by measuring the growth rate of structure in the distribution of galaxies as function of redshift, one can place constraints on gravity, and test if dark energy could be due to deviations from GR [20].

In order to address these discrepancies, a reasonable solution is recently introduced as a novel mechanism beyond the canonical Λ CDM model. This modification to dark energy, which is treated as a smooth non-clustering perfect fluid, may directly interact with dark matter without gravity action. Such an idea has been extensively investigated by a number of phenomenological models, which show that the interaction between DE and DM can alleviate the coincidence problem, and the model predictions have been passed various observational tests. In particular, many parameterized models assume dynamical couplings between DE and DM, and show that the current observational measurements support a nonzero interplay behavior for the cosmic dark sector [21–

*Electronic address: kjg@nao.cas.cn

[33]. Generally, these dynamical coupling scenarios are described with a functional coupling term Q . In this paper, we propose two novel coupling scenarios of DE and DM, and then put constraints on the relevant parameters within the coupling model Q_1 and Q_2 with the help of mainstream cosmological the combination of datasets and finally we research the impact of two interaction models on the C_ℓ^{TT} and matter power $P(k)$ spectra on large scale of universe. Beyond that, we comment on different the neutrino mass hierarchy problem [34–36], i.e. either $m_1 < m_2 \ll m_3$, normal hierarchy(NH) or $m_3 \ll m_1 < m_2$, inverse hierarchy(IH) and analyse the ratios with Λ CDM when setting $\Sigma m_\nu = 0.06eV$ and comment on some crucial hints about the neutrino mass splittings can be demonstrated when investigating these IDE models with the current cosmological observations. From the viewpoint of phenomenology, the given assumptions made for Q function should be tested with a number of cosmological probes [37].

This paper is structured as follows: The scenarios of the interaction IDE1 and IDE2 in dark sector we propose are introduced and from which we derive the relevant evolution equations in Section II. In Section III, we present the SN Ia, BAO, CMB and H(z) data combinations adopted in this work as well as the analysis method in each fitting process with these datasets. The eventual results about the parameters and the C_ℓ and $P(k)$ spectra are obtained from the IDE1 and IDE2 models in Section IV. Finally, we draw our conclusions on two interacting schemes in Section V. We use natural units throughout $c = 8\pi G = 1$.

II. THE MODEL OF THE INTERACTION IN DARK SECTOR

Considering a homogeneous and isotropic Universe with a spatially flat Friedmann-Lematre-Robertson-Walker(FLRW) spacetime whose line element follows the form:

$$ds^2 = -dt^2 + a^2(t) (dr^2 + r^2 d\theta^2 + r^2 \sin^2\theta d\phi^2), \quad (1)$$

where $a(t)$ is cosmic scale factor, t is cosmic time and (r, θ, ϕ) is comoving spherical coordinate system. For a uncoupled standard cosmological model (SM) usually contains radiation, baryons, dark matter and dark energy, their perfect fluid energy-momentum tensor satisfies $T_{\mu\nu} = pg_{\mu\nu} + (\rho + p)U_\mu U_\nu$ respectively, where $U_{\mu,\nu}$ stands for four velocity vector. When introducing the directly interaction of dark constituents, one can understand the conservation equation of total energy momentum tensor as $\nabla_\mu(T_c^{\mu\nu} + T_d^{\mu\nu}) = 0$ based on the Einstein's field equation $G_{\mu\nu} = T_{\mu\nu}^c + T_{\mu\nu}^d$, c, d denotes dark matter and dark energy while the radiation and baryons independently evolve as own mode, respectively. Thus, the FLRW evolution equation for this framework can be written as

$$3H^2 = \rho_d + \rho_c, \quad (2)$$

$$2\dot{H} + H^2 = -p_d, \quad (3)$$

where an overdot refers to a derivative w.r.t the cosmic time t , $H = \dot{a}/a$ is the Hubble parameter, ρ_c, ρ_d are the matter density of dark matter and dark energy and p_c, p_d represents the corresponding pressure of dark matter and dark energy, respectively. Dark matter is usually treated as a pressureless dust matter, $p_c = 0$ while dark energy is taken as a negative pressure fluid $p_d = w_d \rho_d$ with the effective equation of state(EoS) w_d . For instance, if the DE is the smooth vacuum or Λ , i.e. $w_d = -1$. The physical behavior of the effective dark fluid when the presence of interaction in dark sector will be different in light of the sign of the coupling function Q . Thus, the whole energy conservation equation for the interaction can be read as the following forms:

$$\dot{\rho}_c + 3H(1 + w_c^{eff})\rho_c = Q \quad (4)$$

$$\dot{\rho}_d + 3H(1 + w_d^{eff})\rho_d = -Q \quad (5)$$

For a interacting dark fluid of Universe, the sign and strength of the coupling function $Q \neq 0$ determines the effective rate of energy conversion between DM and DE. In the case of $Q < 0$, meaning that the energy transfer from dust DM to DE, while for $Q > 0$, oppositely which implies the DE likewise decay into pressureless DM. As a phenomenological model, it is usually assumed that the interaction term Q is proportional to the product of energy density of a dark fluid and the Hubble parameter, $Q \propto \rho_x H$. Conventionally, the coupling strength Q can be tested by a number of observational results with a linear dependence on the energy density of dark elements as presented in the mathematical formula [38–43]:

$$Q = 3H(\alpha_c \rho_c + \alpha_d \rho_d), \quad (6)$$

where α_c and α_d are dimensionless constants dominating the strength of the DM-DE interaction. In absence of the interaction, namely $Q = 0$, the model restore to Λ CDM cosmology. The redshifted energy density evolution

equations for any coupling term Q and the effective EoS w^{eff} for dark sector can be deduced as:

$$\rho_c = \rho_{c0} \left[\int_{a_0}^a \left(\frac{Q}{aH} \right) da \right], \quad (7)$$

$$\rho_d = \rho_{d0} \left[a^{-3(1+w_d)} - \int_{a_0}^a \left(\frac{Q}{aH} \right) da \right], \quad (8)$$

$$w_c^{eff} = \frac{Q}{3H\rho_c}, \quad w_d^{eff} = w_d - \frac{Q}{3H\rho_d}, \quad (9)$$

where w_c^{eff} and w_d^{eff} are respectively termed as the effective equation of state for CDM and DE, ρ_{c0} and ρ_{d0} denote cold dark matter and dark energy current matter density, and a_0 is today cosmic factor, Q stands for any coupling function of dark sector, respectively,

The origin of instabilities depend on different signs of α_c and α_d and effective EoS w^{eff} under the interacting dark energy (IDE) scenarios[44–49]. In this work, we propose originally two interacting scenarios as following physical mechanism: in which the coupling function $Q(t)$ can be defined as:

$$IDE1 : Q_1 = 3H\alpha\rho_d \left[1 + \beta \ln \left(1 - \frac{\rho_c}{\rho_d} \right) \right], \quad (10)$$

$$IDE2 : Q_2 = 3H\alpha\rho_d \left[1 + \beta \sin \left(\frac{\rho_c}{\rho_d} \right) \right], \quad (11)$$

where α and β are dimensionless coupling parameter governing the interaction strength of the dark sector and then one can expands Q function around the $\rho_c/\rho_d = 1$ in the manner of Taylor series and the first order approximation we take for the interaction model IDE1 and IDE2 and thus Q_1 and Q_2 can be rewritten as a non-linear expression:

$$Q_1 \approx 3H\alpha\rho_d \left(1 - \frac{\beta\rho_c}{\rho_d} \right) = 3H\alpha(\rho_d - \beta\rho_c), \quad (12)$$

and

$$Q_2 \approx 3H\alpha\rho_d \left(1 + \frac{\beta\rho_c}{\rho_d} \right) = 3H\alpha(\rho_d + \beta\rho_c), \quad (13)$$

Then we further derive the effective EoS Eq.9 in term of above interaction function via $r = \rho_c/\rho_d$ for IDE1 model:

$$w_c^{eff} = \alpha \left(\frac{1}{r} - \beta \right), \quad w_d^{eff} = w_d - \alpha(1 - \beta r), \quad (14)$$

meanwhile for IDE2:

$$w_c^{eff} = \alpha \left(\frac{1}{r} + \beta \right), \quad w_d^{eff} = w_d - \alpha(1 + \beta r), \quad (15)$$

Fig.1 shows the evolution behavior of w_c^{eff} and w_d^{eff} with respect to redshift z for the two interaction schemes Q_1 and Q_2 , respectively. The left panel of Fig.1 displays the evolution of w_c^{eff} as well as the evolution of w_d^{eff} in the right panel taking same values of the α and β for IDE1 as well as IDE2 when fixing $w_d = -0.99$, one can find the effective equations of state for dust DM and DE are sensitive to the interaction parameter α and β and the evolution of w_c^{eff} and w_d^{eff} for IDE1 and IDE2 maintain stable for $z > 1.5$ around the $w_d = -1$ from the picture. As for IDE1 we see, the energy transition occurs from DM to DE $Q < 0$ ($\alpha < 0$ and $\beta > 0$) while $Q > 0$ ($\alpha > 0$ and $\beta < 0$) energy flows from DM to DE after $z > 0.5$, while for IDE2 case, the energy flows between DE and DM opposite direction compared to IDE1 case in term of the various sign of α and β .

Now, the main perturbative equations of energy density δ and velocity v under the any interaction Q of DE and DM model in synchronous gauge for dark energy become [38, 50–57]:

$$\delta'_d = \frac{a}{\rho_d} Q_d - \frac{aQ}{\bar{\rho}_d} \left[\delta_d + 3\mathcal{H} \left(c_{(s)d}^2 - w_d \right) \delta v \right], \quad (16)$$

$$v'_d = \frac{aQ}{\bar{\rho}_d} \left[v_d - \left(1 + c_{(s)d}^2 \right) v_d \right] - \frac{a}{\rho_d} \left[\frac{c_{(s)d}^2 \rho_d}{a} \delta_d - Qv \right]. \quad (17)$$

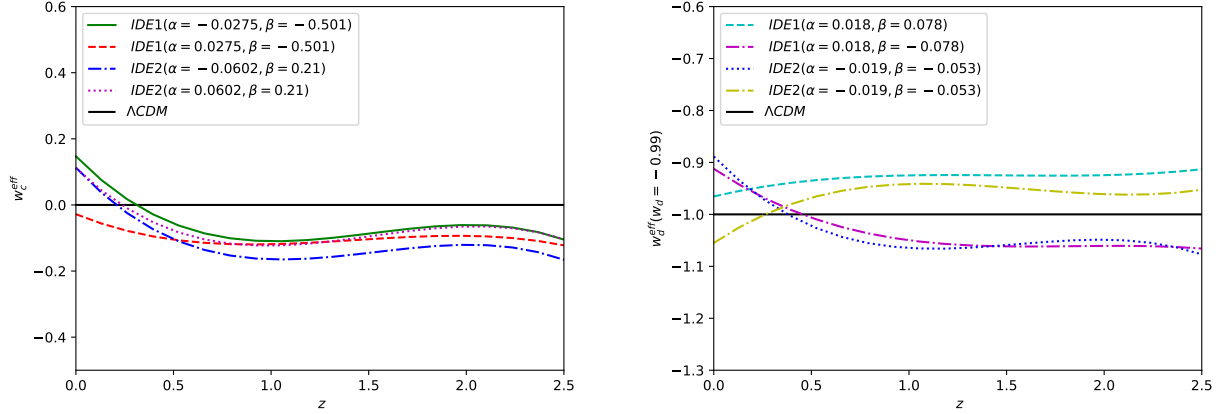


FIG. 1: The figure shows the redshift evolution of the effective equations of state for DE(top) and CDM (below) under the interaction models Q_1 and Q_2 when taking different two groups value for α and β , respectively.

Similarly, as for the cold dark matter perturbations, $w_c = 0$ leading to $c_{(a)c}^2 = c_{(s)c}^2 = 0$, its perturbative formula of energy δ'_c and speed v'_c can be read respectively as:

$$\delta'_c = k^2 v_c - \frac{h'}{2} - \frac{a}{\bar{\rho}_c} Q + \frac{aQ}{\bar{\rho}_c} \delta_c. \quad (18)$$

$$v'_c = -\mathcal{H}v_c - \frac{aQ}{\bar{\rho}_c} (v - v_c). \quad (19)$$

here $\delta_i = \delta\rho/\rho$ ($i = c, d$) and $\mathcal{H} = aH$ is comoving Hubble parameter.

Besides, we discuss the contribution of matter overdensity δ that resulted from the interaction between dark energy and dark matter. In term of the general definition of the growth rate of matter perturbations: $f_c = \frac{d \ln \delta_c}{d \ln a} = \delta'/\delta_c$ and for an arbitrary interaction function Q [30, 58, 59], the growth rate can be understood as:

$$\delta''_c + \left(1 - \frac{Q}{H\rho_c}\right) \mathcal{H}\delta'_c = \frac{3}{2} \mathcal{H}^2 \Omega_b \delta_b + \frac{3}{2} \mathcal{H}^2 \Omega_c \delta_c \left\{ 1 + \frac{2\rho_d}{3\rho_c} \frac{Q}{H\rho_c} \left[\frac{\mathcal{H}'}{\mathcal{H}^2}, +1 - 3w_d + \frac{w_d}{\mathcal{H}(1+w_d)} + \frac{Q}{H\rho_c} \left(1 + \frac{\rho_d}{\rho_c}\right) \right] \right\}, \quad (20)$$

It's difficult to solve the analysis expression of f_c in Eq.20 but we can fit it using the format $f_c(z) = \Omega_m^\gamma$ ($\gamma \approx 0.55$ in Λ CDM cosmology [60, 61]) with observations combinations as shown in Fig.2 and from the plot, we find that growth formation of the CDM is much sensitive to various interaction model Q and coupling factors especially after redshift $z = 2$ when DE begins to dominate cosmic energy ingredient and drives the accelerated expansion of the universe .

In this work, we investigate cosmological dynamics with the flat spacetime due to the above Eqs.1–13, neglecting the radiation density $\Omega_{r0} \approx 10^{-5}$, therefore assuming the matter density relation $\Omega_m + \Omega_d = 1$ for IDE1 case can be rewritten:

$$H(z)^2/H_0^2 = \Omega_d \left(\frac{w}{\alpha + \beta} (1+z)^3 + \frac{1}{\alpha + \beta} (1+z)^{3(1+w+\alpha)} \right) + \Omega_m (1+z)^3, \quad (21)$$

For the IDE2 scheme:

$$H(z)^2/H_0^2 = \Omega_m \left(\frac{w}{\alpha + \beta} (1+z)^{3(1+w)} + \frac{1}{\alpha + \beta} (1+z)^{3(1-w-\alpha)} \right) + \Omega_d (1+z)^{3(1+w)} \quad (22)$$

where Ω_m and Ω_d are current energy density of dark matter and dark energy.

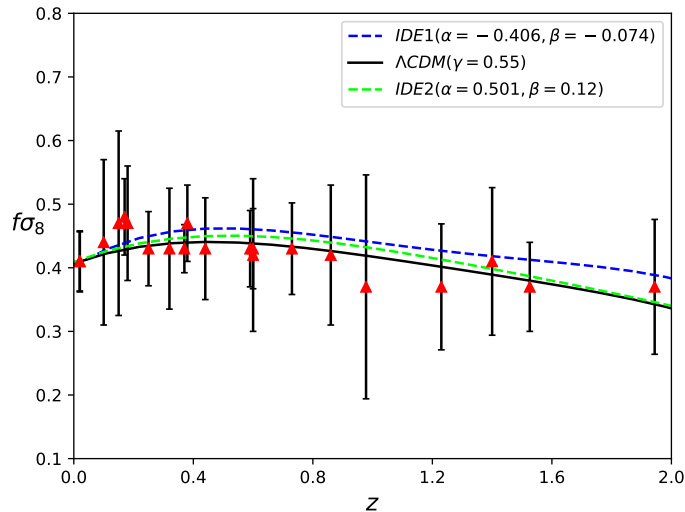


FIG. 2: The linear evolution of $f\sigma_8$ as the function of redshift z for interaction models Q_1 and Q_2 (dash blue and lime line, black solid line stands for Λ CDM model, respectively). Errorbar datapoints are employed in Table I of [62]

III. DATA AND METHODOLOGY

In this section we introduce the mainstreams cosmological probes and the likelihood function $\mathcal{L} \propto e^{-\chi^2/2}$ used in this work to extract the posterior distribution functions (PDFs) of each parameter within IDE1 and IDE2 framework.

A. SN Ia data

The Type Ia Supernovae (SN Ia) play a key role in unveiling the character of the dark energy as the "standard candles". We utilize the Pantheon compilation consisting of 1048 SN Ia samples covering redshift range $0.01 < z < 2.3$ [63]. The χ^2 distribution for the SN Ia can be written as

$$\chi_{\text{SN}}^2 = \Delta \mathbf{u}^T \cdot \mathbf{C}^{-1} \cdot \Delta \mathbf{u}. \quad (23)$$

Here $\Delta \mathbf{u} = \mathbf{u}_{\text{obs}} - \mathbf{u}_{\text{th}}$, \mathbf{u}_{obs} and \mathbf{u}_{th} are the vectors of observational and theoretical distance modulus, respectively, and \mathbf{C} is the covariance matrix. $u_{\text{th}} = m_{\text{th}} - M$, where u_{th} is the theoretical apparent magnitude, it can be obtained as

$$u_{\text{th}} = 5 \log_{10} D_L(z) + 25, \quad (24)$$

where M is the absolute magnitude of SN Ia as a nuisance parameter, $D_L(z) = (1+z)D_C(z)$ is the luminosity distance in unit of Mpc . The covariance matrix \mathbf{C} takes the form as

$$\mathbf{C} = \mathbf{C}_{\text{stat}} + \mathbf{C}_{\text{sys}}, \quad (25)$$

where \mathbf{C}_{stat} is the vector of statistic error, \mathbf{C}_{sys} is the systematic covariance matrix for the data [63].

B. BAO data

Table I lists the adopted quantities that derived from the different BAO measurements as the "standard ruler", r_s is the radius of the comoving sound horizon at the drag epoch as following:

$$r_s = \int_0^{t_s} c_s \frac{dt}{a}, \quad (26)$$

TABLE I: The 12 BAO data used in this work redshift from $z = 0.1$ to 2.4 .

Redshift	Measurement	Value	$r_{s,\text{fid}}$	Survey	Reference
0.106	r_s/D_V	0.3360 ± 0.015	–	6dFGS	[64]
0.15	r_s/D_V	0.2239 ± 0.0084	–	SDSS DR7	[65]
0.32	r_s/D_V	0.1181 ± 0.0024	–	BOSS LOW-Z	[66]
0.57	r_s/D_V	0.0726 ± 0.0007	–	BOSS CMASS	[67]
0.44	r_s/D_V	0.0870 ± 0.0042	–	WiggleZ	[68]
0.60	r_s/D_V	0.0672 ± 0.0031	–	WiggleZ	[68]
0.73	r_s/D_V	0.0593 ± 0.0020	–	WiggleZ	[68]
2.34	r_s/D_V	0.0320 ± 0.0013	–	SDSS-III DR11	[69]
2.36	r_s/D_V	0.0329 ± 0.0009	–	SDSS-III DR11	[70]
0.38	$D_M(r_{s,\text{fid}}/r_s)$	1518 ± 22	147.78	SDSS DR12	[71]
0.51	$D_M(r_{s,\text{fid}}/r_s)$	1977 ± 27	147.78	SDSS DR12	[71]
2.40	D_H/r_s	8.94 ± 0.22	–	SDSS DR12	[72]

where c_s is the sound speed, t_s is the epoch of last scattering, a is the scale factor. Since r_s are not sensitive to physics at low redshifts, we fix $r_s = 147.09 \pm 0.26$ measured from the Planck 2018 release [13]. The spherically averaged distance D_V is given by

$$D_V(z) = \left[D_M^2(z) \frac{cz}{H(z)} \right]^{1/3}, \quad (27)$$

where $D_M(z) = (1+z)D_A$ is the comoving angular diameter distance, and $D_A = D_C/(1+z)$ is the physical angular diameter distance. $D_H = c/H(z)$ is the Hubble distance.

The χ^2 for the BAO data can be calculated by

$$\chi_{\text{BAO}}^2 = \Delta \mathbf{D}^T \cdot \mathbf{C}_D^{-1} \cdot \Delta \mathbf{D}, \quad (28)$$

where $\Delta D = \mathbf{D}_{\text{obs}} - \mathbf{D}_{\text{th}}$, \mathbf{D}_{obs} and \mathbf{D}_{th} are the observational and theoretical quantities shown in Table . I and \mathbf{C}_D is corresponding covariance matrix.

C. CMB data

For the CMB dataset, we exploit the parameter of acoustic scale ℓ_A , the shift parameter R , the decoupling redshift z_* inferred from the Planck CMB measurement and the distance priors from the Planck 2018 results [13, 73], they are defined respectively as

$$R = \sqrt{\Omega_m H_0^2 r(z_*)}, \quad (29)$$

$$\ell_A = \pi r(z_*)/r_s(z_*), \quad (30)$$

where Ω_m is current energy density of dark matter. $r(z_*)$ is the comoving size of the sound horizon at the redshift of the decoupling epoch of photons z_* , z_* can be expressed as [74–76]:

$$z_* = 1048[1 + 0.00124(\Omega_b h^2)^{-0.738}][1 + g_1(\Omega_m h^2)^{g_2}], \quad (31)$$

where

$$g_1 = \frac{0.0783(\Omega_b h^2)^{-0.238}}{1 + 39.5(\Omega_b h^2)^{0.763}}, g_2 = \frac{0.560}{1 + 21.1(\Omega_b h^2)^{1.81}}. \quad (32)$$

The χ^2 distribution for the CMB data can be estimated as

$$\chi_{\text{CMB}}^2 = \Delta \mathbf{X}^T C_{\text{CMB}}^{-1} \Delta \mathbf{X}, \quad (33)$$

where $\omega_b = \Omega_b h^2$ is the baryon energy density, h is the dimensionless Hubble constant. $\Delta X = \mathbf{X}_{\text{obs}} - \mathbf{X}_{\text{th}}$, $\mathbf{X} = (\mathbf{R}, \ell_A, \omega_b)$ and C_{CMB} is the covariance matrix.

TABLE II: The table lists the priors on the parameters space.

Parameter	Prior range
Ω_m	[0, 0.7]
h	[0.5, 1]
α	[-1, 1]
β	[-1, 1]
w_d^{eff}	[-3,-0.3]
σ_8	[0.2,1.4]

TABLE III: The table summarizes the mean values and 1- σ (68.3%) uncertainties of the parameters under the scenario of the IDE1: $Q_1 = 3H\alpha\rho_d(1 + \beta\ln(1 - \frac{\rho_c}{\rho_d}))$ case in Fig.3. Here the parameter Ω_m equal the energy fractions of baryons plus dark matter, i.e. $\Omega_m = \Omega_c + \Omega_b$.

Parameter	CMB	CMB+SN Ia	CMB+BAO+H(z)	CMB+SN Ia+BAO+H(z)
Ω_m	$0.322^{+0.01}_{-0.009}$	$0.303^{+0.007}_{-0.007}$	$0.297^{+0.008}_{-0.008}$	$0.298^{+0.006}_{-0.006}$
h	$0.677^{+0.007}_{-0.008}$	$0.726^{+0.0061}_{-0.0067}$	$0.691^{+0.007}_{-0.007}$	$0.684^{+0.0051}_{-0.006}$
α	$-0.457^{+0.005}_{-0.005}$	$-0.465^{+0.004}_{-0.004}$	$-0.47^{+0.004}_{-0.004}$	$-0.468^{+0.003}_{-0.004}$
β	$0.861^{+0.012}_{-0.014}$	$0.886^{+0.013}_{-0.012}$	$0.876^{+0.013}_{-0.013}$	$0.874^{+0.013}_{-0.013}$
w_d^{eff}	$-0.986^{+0.026}_{-0.189}$	$-1.005^{+0.019}_{-0.019}$	$-1.006^{+0.027}_{-0.024}$	$-1.015^{+0.020}_{-0.022}$
σ_8	$0.811^{+0.01}_{-0.009}$	$0.814^{+0.008}_{-0.009}$	$0.827^{+0.01}_{-0.01}$	$0.822^{+0.01}_{-0.01}$
χ_{red}^2	0.989	1.067	1.173	1.114

D. H(z) Data

The $H(z)$ data contain 30 data points in the redshift range from 0 to 2 in Table 4 of [77], which are obtained using the differential-age method, that is to compare the ages of passively-evolving galaxies with similar metallicity, separated in a small redshift interval [78] serving as cosmic chronometers and yielding a model-independent measurement of the expansion rate of the Universe at various redshifts. The χ^2 distribution for the $H(z)$ data can be expressed as [75, 76]

$$\chi_H^2 = \sum_{i=1}^{N=30} \frac{[H_{\text{obs}}(z_i) - H_{\text{th}}(z_i)]^2}{\sigma_H^2}. \quad (34)$$

Here H_{obs} and H_{th} are the observational and theoretical Hubble parameters, respectively, and σ_H is the error.

Finally, the joint χ^2 of above four datasets employed in this work can be calculated by

$$\chi^2 = \chi_{SN}^2 + \chi_{BAO}^2 + \chi_{CMB}^2 + \chi_{H(z)}^2. \quad (35)$$

IV. RESULTS

In order to analyse the IDE1 and IDE2 model introduced in Sec.II and place constraints on the free parameters within the scenarios, we use CMB data and the combination of CMB+Pantheon, CMB+BAO+H(z), and CMB+Pantheon++BAO+H(z) datasets and modify the Boltzmann code CLASS [79]¹ to solve the background and perturbation equations of IDE1 and IDE2 model and then we utilize MontePython, a Markov chain Monte Carlo package (MCMC)[80–82]² with the Metropolis-Hastings algorithm in accordance with the Gelman-Rubin convergence criterion, requiring $|R - 1| < 0.01$ to extract the chains of each parameter by computing the reduced chi-square $\chi_{red}^2 = \chi_{min}^2/(N - n)$ in the fitting process for each dataset combination, where χ_{min}^2 is the minimum

¹ https://github.com/lesgourg/class_public

² https://github.com/brinckmann/montepython_public

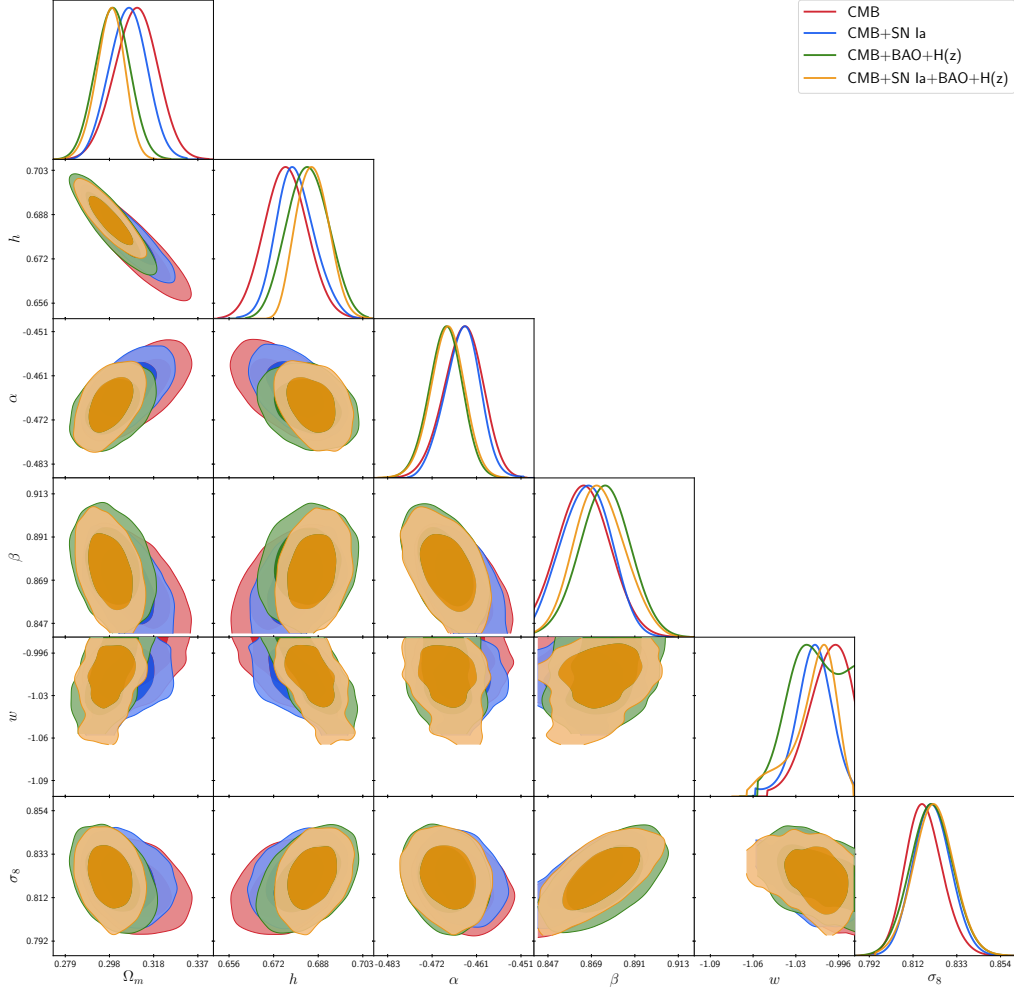


FIG. 3: The one-dimensional posterior distributions and two-dimensional contours in $1\text{-}\sigma$ (68.3%) and $2\text{-}\sigma$ (95.5%) confidence level (C.L.) of the free parameters for the $Q_1 = 3H\alpha\rho_d(1 + \beta\ln(1 - \frac{\rho_c}{\rho_d}))$ interacting dark energy scenario. The red, blue, green, and orange plots stand for the constraint results from CMB, CMB+SN Ia, CMB+BAO+H(z) and joint datasets, respectively.

χ^2 , N and n are the number of data point and free parameter, respectively. The priors on the parameter space are shown in Table.II.

Firstly, Fig.3 and Fig.4 show the 68.3% and 95.5% confidence level (C.L.) contour map and 1-D PDFs of the free parameter of IDE1: $Q_1 = 3H\alpha\rho_d(1 + \beta\ln(1 - \frac{\rho_c}{\rho_d}))$ and IDE2: $Q_2 = 3H\alpha\rho_d(1 + \beta\sin(\frac{\rho_c}{\rho_d}))$ models explored by using CMB and CMB+SN Ia and CMB+BAO+H(z) and joint datasets respectively because of these datasets can break the degeneracy of the among quantities. We find that the model can be constrained by these datasets well due to χ_{red}^2 is close to 1 for the above four data combinations. As listed on table III, the best-fit value of the coupling factor α and β in Fig 3 yield $\alpha \simeq -0.468^{+0.003}_{-0.004}$ and $\beta \simeq 0.874^{+0.013}_{-0.013}$ for the joint datasets and the $Q_1 \approx -0.00002H(z) < 0$ manifests a difference from zero, i.e. energy transfers from dark matter into dark energy. In addition, the equation of state $w_d^{eff} < -1$ for DE is preferred from the fitting consequences of CMB+SN Ia+BAO+H(z) combination. The results of other cosmological parameters from the fitting are also perfectly consistent with observational values. Otherwise, concerning Fig.4 and Table.IV present the results of IDE2: $Q_2 = 3H\alpha\rho_d(1 + \beta\sin(\frac{\rho_c}{\rho_d}))$ scenario, the mean values of the interaction factors $\alpha \simeq -0.866$ and $\beta \simeq 0.775$ and so $Q_2 \approx 0.00004H(z) > 0$ meaning the dark energy decays into dark matter in light of the results from observational dataset combinations.

Furthermore, we analyse either issues of H_0 tension or the σ_8 discrepancy [16, 83] mentioned in Section.I and both issues can be slightly alleviate due to the constraints values under the two interacting IDE1 and IDE2 framework. From Table.III we see, the IDE1 model gives the dimensionless Hubble constant h from 0.666 to

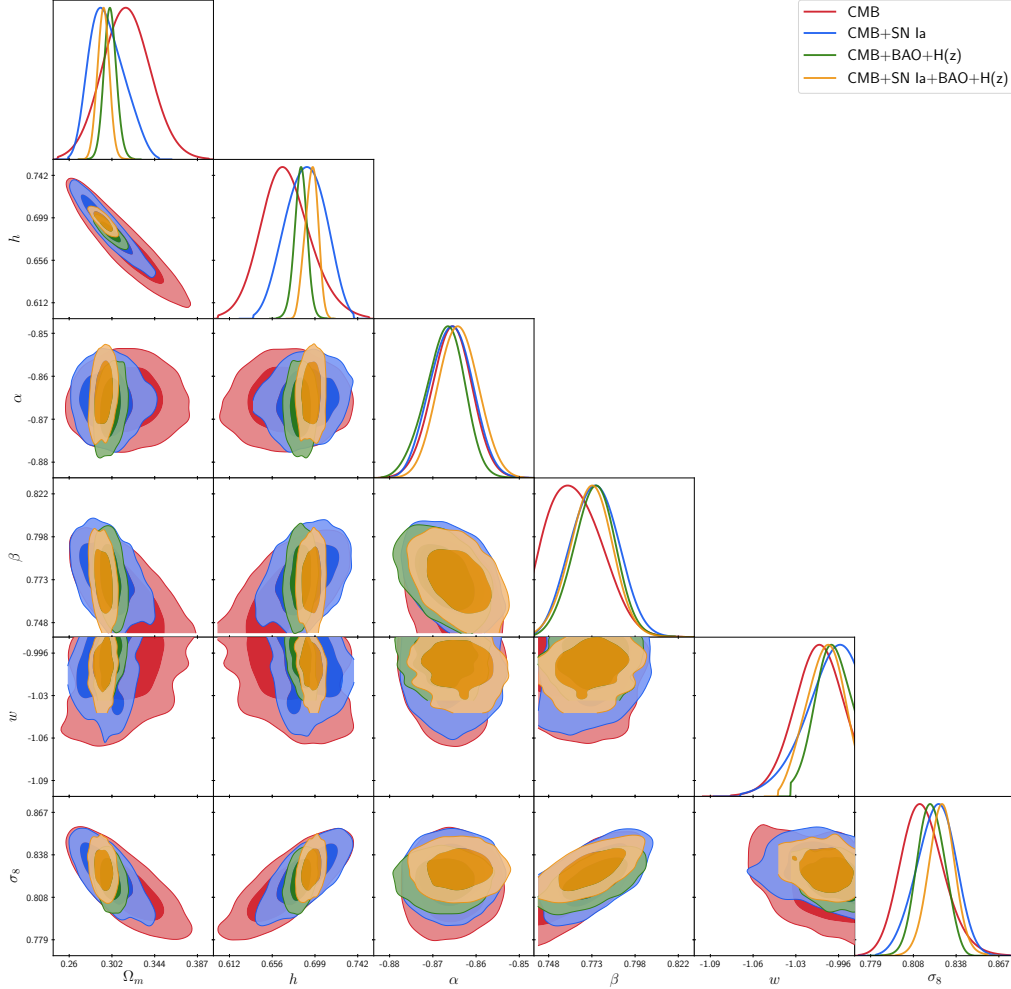


FIG. 4: The one-dimensional posterior distributions and two-dimensional contours in 1- σ (68.3%) and 2- σ (95.5%) confidence level(C.L.) of the free parameters for the $Q_2 = 3H\alpha\rho_d(1 + \beta\sin(\frac{\rho_c}{\rho_d}))\rho_c$ interacting dark energy scenario. The red, blue, green, and orange plots show the constraint results from CMB, CMB+SN Ia, CMB+BAO+H(z) and joint datasets, respectively.

0.686 using the four data combinations, which are almost consistent in 1σ level and similarly, the resulting values σ_8 are tightly obtained from 0.811 to 0.827. While in the IDE2 model, the tensions are also decreased to some extent, the values of h and σ_8 show no serious deviation from the CMB data only to the joint dataset fitting. In short, these results of parameters from solely Planck CMB data to four observations combinations imply that the non-linear interactions of DE and DM considered in this work can be supported well by the available observational data which determined from Λ CDM cosmology.

In order to further understand the relation between the coupling factor α and β and the time of matter-radiation equality for the existing of an interaction in cosmic dark sector, we draw the evolution curves of Ω_m/Ω_r in redshift space z , the time of matter-radiation equality comes later in both IDE1 and IDE2 case with increasing value of α and β around redshift $z=3400$ to 3500 compared to non-interacting model as shown in Fig.5, indicating the increasing of interaction parameter α and β will lead to a addition of energy density of the dust matter Ω_m , the epoch of matter-radiation balance will become late and the sound horizon will scales up.

Fig.6 presents some key signatures on the CMB temperature power spectrum in left and the linear matter power spectrum in right panel when taking the different values for α and β describing interacting models IDE1 and IDE2. Concerning the CMB temperature power spectra in the left panel, we deem that actually either dark energy or dark matter gains additional energy density and influences the microwave background temperature anisotropy especially at low multiple $l < 30$ under the IDE1 and IDE2 respectively. The increase of dark energy density within IDE1 compared to IDE2, especially alters integrated Sachs-Wolfe(ISW) level on large scale due to the decay of gravitational potential over expansion history as well as changes era of matter-radiation balance

TABLE IV: The table shows mean values and 1- σ (68.3/%) confidence level(C.L.) of the cosmological parameters under the IDE2: $Q_2 = 3H\alpha\rho_d(1 + \beta\sin(\frac{\rho_c}{\rho_d}))$ case in Fig.4 fitted by above datasets,here $\Omega_m = \Omega_c + \Omega_b$.

Parameter	CMB	CMB+SN Ia	CMB+BAO+H(z)	CMB+SN Ia+BAO+H(z)
Ω_m	$0.317^{+0.025}_{-0.022}$	$0.298^{+0.015}_{-0.018}$	$0.300^{+0.006}_{-0.007}$	$0.294^{+0.006}_{-0.006}$
h	$0.680^{+0.022}_{-0.028}$	$0.701^{+0.020}_{-0.020}$	$0.694^{+0.006}_{-0.006}$	$0.686^{+0.006}_{-0.006}$
α	$-0.866^{+0.0049}_{-0.0049}$	$-0.866^{+0.005}_{-0.005}$	$-0.867^{+0.0047}_{-0.0045}$	$-0.864^{+0.005}_{-0.005}$
β	$0.765^{+0.011}_{-0.019}$	$0.775^{+0.014}_{-0.013}$	$0.775^{+0.013}_{-0.012}$	$0.7727^{+0.012}_{-0.013}$
w_d^{eff}	$-1.005^{+0.019}_{-0.017}$	$-0.995^{+0.024}_{-0.027}$	$-0.998^{+0.018}_{-0.013}$	$-1.007^{+0.016}_{-0.013}$
σ_8	$0.815^{+0.013}_{-0.017}$	$0.8236^{+0.014}_{-0.013}$	$0.820^{+0.009}_{-0.009}$	$0.8278^{+0.009}_{-0.009}$
χ^2_{min}	0.973	1.082	1.154	1.203

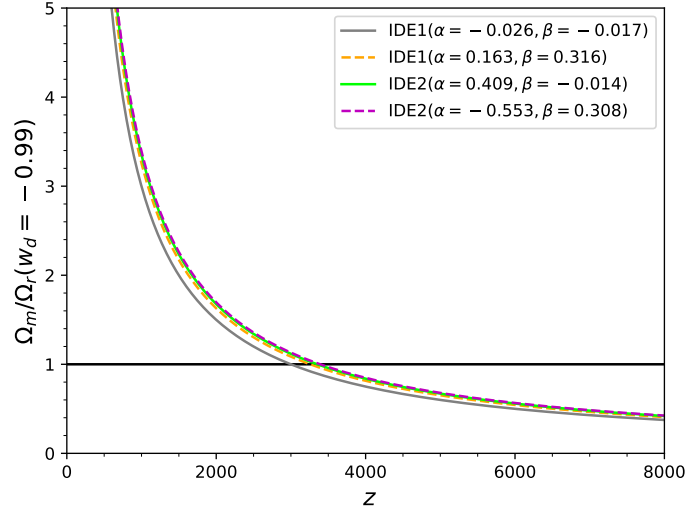


FIG. 5: The evolution for the ratio of matter and radiation Ω_m and Ω_r with the variation of the interaction parameter α and β for IDE1 and IDE2, here $\Omega_m = \Omega_c + \Omega_b$. The horizontal gray thick line corresponds to the case of $\Omega_m = \Omega_r$, namely the era of the matter-radiation equality and we fix these parameters for the plot $\Omega_m = 0.278, \Omega_b = 0.04, \Omega_d = 0.682, \Omega_r = 0.00005$.

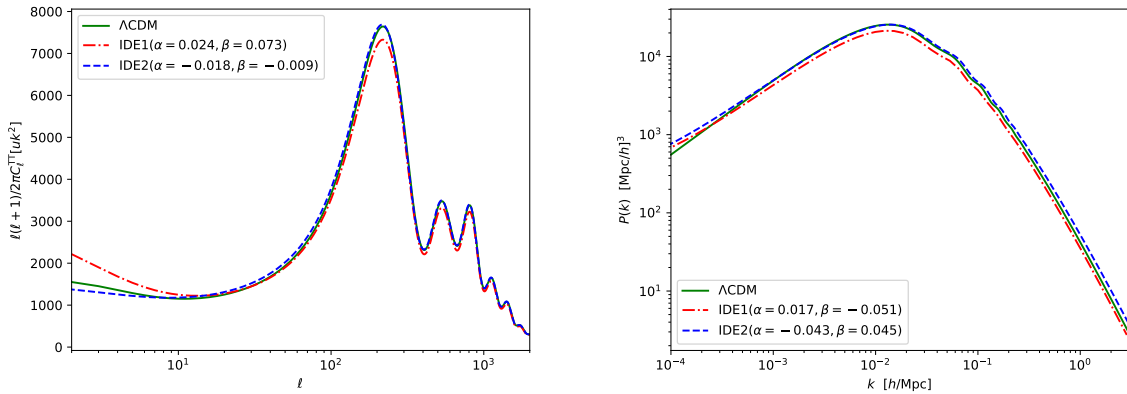


FIG. 6: The effects on the CMB temperature power spectra(left panel) and the matter power spectra (right panel)for two case of the interaction term Q_1 and Q_2 . The red and blue curves lines for the IDE1: Q_1 and IDE2: Q_2 reference to Λ CDM in green solid line, respectively.

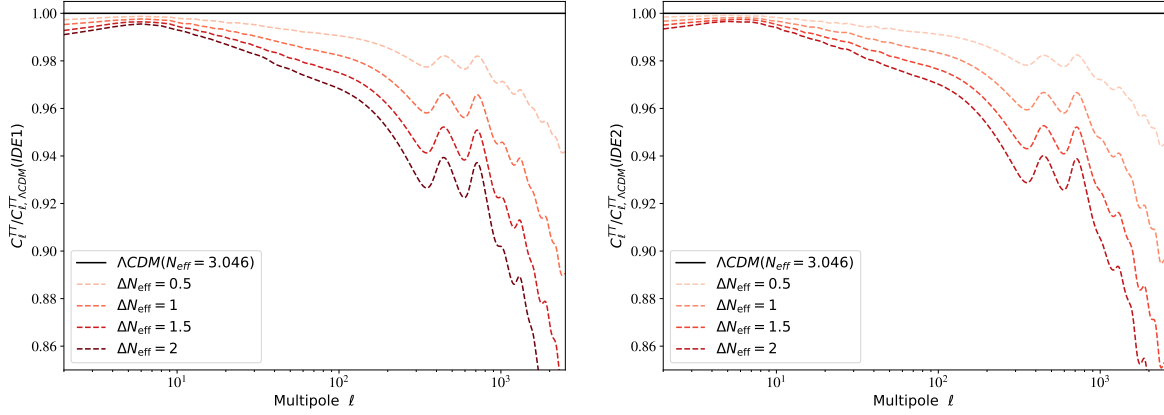


FIG. 7: The ratio of the CMB temperature power spectra to Λ CDM in presence of neutrino for the interaction term IDE1(left panel) and IDE2(right panel) with the variation of ΔN_{eff} from 0.5 to 2.

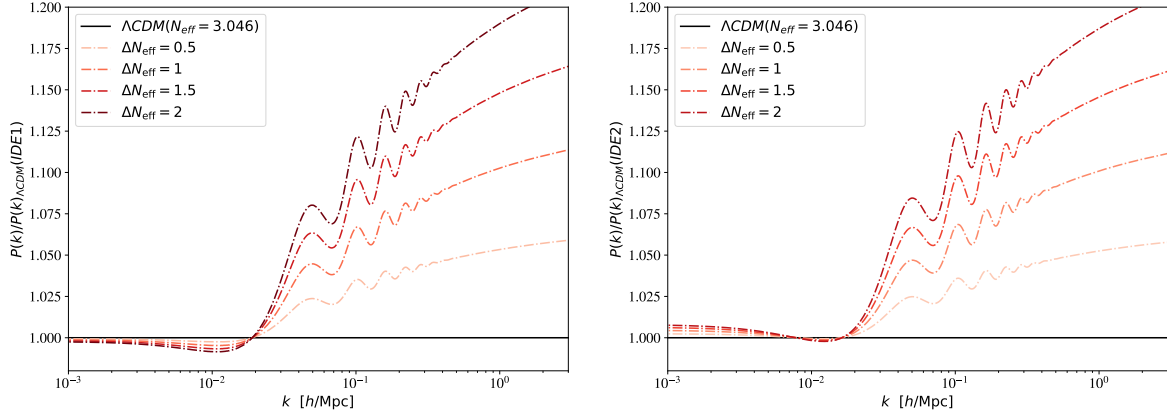


FIG. 8: The ratio of the matter power spectra to Λ CDM of the interaction term IDE1(left panel) and IDE2(right panel) when ΔN_{eff} from 0.5 to 2.

and the height of the first peak of CMB temperature power spectra is lifted for the tight coupling of dark sector. As for the right panel, the dominant effects on the linear matter power spectrum $P(k)$ show up at large scales ($k < 0.042h/Mpc$), hinting the enhancement of the content of dark matter that forms larger cosmic structures and earlier matter clusters of galaxies under its gravity. Consequently, the shape of matter power spectra $P(k)$ somewhat is more intensified due to larger horizon boundary in IDE2 than IDE1 model. Moreover, the first peak evidently is risen for IDE1 in small multipole $\ell \lesssim 10$ since the dark energy fluid flows to dark matter to change the energy of CMB photons when across it. The presence of interaction of dark sector changes the regular evolution law and which is imprinted on the integrated Sachs-Wolfe (ISW) effect in large scale effect of the CMB TT spectrum.

In this paragraph, we comment on neutrino hierarchies problem under the framework IDE1 and IDE2 model. The experiment of neutrino oscillation has suggested that neutrinos have mass size and mass splittings among three flavors neutrino, though either absolute mass of neutrinos or mass hierarchies remain puzzling (see [31, 34, 35, 37, 84] for a review). Actually, both the properties of massive neutrinos and dark energy could imprint important signatures on expansion history and large scale structure (LSS) in the evolution history of the universe [35, 36, 85, 86, 86]. Therefore, It's expected that some significant information can be found on C_ℓ and $P(k)$ spectrum in the direct interaction of dark energy and dark matter scenario when considering mass hierarchies. From the ratio of C_ℓ^{TT} to C_ℓ^{TT} in Λ CDM model in Fig.7, one can find there is mass size and mass hierarchies of neutrino species and showing bigger deviation in IDE1 than IDE2 related to Λ CDM regardless of NH or IH mode and demonstrating the gradual suppression for the larger free degree of $\Delta N_{eff} = N - 3.046$ from 0.5 to 2 occurring in IDE1 and IDE2 due to the smoothing effect of more neutrinos free streaming. Similarly, concerning the ratio of matter power $P(k)/P(k)_{\Lambda\text{CDM}}$ is dramatically intensified in $k > 0.02h/Mpc$ in the

wake of ΔN_{eff} turns bigger from 0.5 to 2 in Fig.8, the attribute of neutrinos may strongly degeneracy with dark matter halos to cluster of baryon particles and host a vast of galaxies or other objects in both IDE1 and IDE2 models, but in $k < 0.02h/Mpc$ phase, the magnitude of ratio amplitude of IDE2 than IDE1 is less than and tend to 1 due to the density of neutrinos are diluted since in larger scales and difficult to cluster.

V. CONCLUSIONS

In this analysis, we have investigated two scenarios of direct interaction between the dark energy and dark matter, in which the interaction term Q is reconstructed as Eq.10 and Eq.11 with coupling parameter α and β determining the conversion between DE and DM.

Firstly, we come up with two novel interacting model IDE1 and IDE2, and then we use (i) the cosmic microwave background from Planck 2018 result, (ii) Pantheon sample of Supernovae Type Ia, (iii) baryon acoustic oscillations distance measurements and (iv) direct $H(z)$ observation to put constraints on the two interacting scenarios $Q_1 = 3H\alpha\rho_d(1 + \beta\ln(1 - \frac{\rho_c}{\rho_d}))$ and $Q_2 = 3H\alpha\rho_d(1 + \beta\sin(\frac{\rho_c}{\rho_d}))$ by calling the MontePython sampler and Class code. All results summarized in Table.III and IV and Fig.3 and 4, we find that

(1) our analysis with all combined datasets support non-zero value for the interacting factors α and β while the dark energy equation of state(EoS) $w < -1$ at 2σ confidence level.

(2) With IDE1 or IDE2 model, we point out that the results from the interactions are compatible with a general model such as the uncoupled w CDM cosmology and fit the latest observations. Specially, it is evident that the interacting models relaxed the existing tensions of H_0 and σ_8 arised from different cosmological measurements relying on the Λ CDM picture at about 2σ confidence level, though it does not seem to be able to completely alleviate them.

(3) When the addition of neutrinos mass normal hierarchy(NH) and inverse hierarchy(IH) mode to the interaction theory of IDE1 and IDE2 scenario, we discuss that the influence on the ratio of CMB temperature spectrum, indicating the neutrinos obviously smooth temperature fluctuation especially in $k > 100$ with the free degree error ΔN_{eff} from 0.5 to 2, while the effect of dark matter to drag baryons particles to cluster and spark the physical processes are reinforced due to the more neutrinos behaving like dark matter to form larger structures of halos.

As a whole, we confirm that the interaction of dark energy and dark matter in this work can be explored by the cosmological observation combinations and eliminate some discrepancies to some extent that from theory and determination and even can produce some key signals on the C_ℓ and $P(k)$ spectrum can be detected in a number of cosmology surveys in future.

Acknowledgment

We thank Tongjie Zhang for constructive comments on the manuscript.

-
- [1] A. G. Riess, A. V. Filippenko, P. Challis, A. Clocchiatti, A. Diercks, P. M. Garnavich, R. L. Gilliland, C. J. Hogan, S. Jha, R. P. Kirshner, et al., *Astron. J.* **116**, 1009 (1998), astro-ph/9805201.
 - [2] S. Perlmutter, G. Aldering, G. Goldhaber, R. A. Knop, P. Nugent, P. G. Castro, S. Deustua, S. Fabbro, A. Goobar, D. E. Groom, et al., *Astrophys. J.* **517**, 565 (1999), astro-ph/9812133.
 - [3] P. J. Peebles and B. Ratra, *Reviews of Modern Physics* **75**, 559 (2003), astro-ph/0207347.
 - [4] E. J. Copeland, M. Sami, and S. Tsujikawa, *International Journal of Modern Physics D* **15**, 1753 (2006), hep-th/0603057.
 - [5] M. Li, X.-D. Li, S. Wang, and Y. Wang, *Communications in Theoretical Physics* **56**, 525 (2011), 1103.5870.
 - [6] C. Wetterich, *Astron. Astrophys.* **301**, 321 (1995), hep-th/9408025.
 - [7] B. Wang, Y. Gong, and E. Abdalla, *Physics Letters B* **624**, 141 (2005), hep-th/0506069.
 - [8] D. Tocchini-Valentini and L. Amendola, *Phys. Rev. D* **65**, 063508 (2002), astro-ph/0108143.
 - [9] L. P. Chimento, A. S. Jakubi, D. Pavón, and W. Zimdahl, *Phys. Rev. D* **67**, 083513 (2003), astro-ph/0303145.
 - [10] P. Rudra, in *41st COSPAR Scientific Assembly* (2016), vol. 41 of *COSPAR Meeting*, pp. H0.2–11–16.
 - [11] H. Paul and M. Pavicic, *Journal of the Optical Society of America B Optical Physics* **14**, 1275 (1997), quant-ph/9908023.
 - [12] I. Zlatev, L. Wang, and P. J. Steinhardt, *Phys. Rev. Lett.* **82**, 896 (1999), astro-ph/9807002.
 - [13] P. Collaboration, N. Aghanim, Y. Akrami, M. Ashdown, J. Aumont, C. Baccigalupi, M. Ballardini, A. J. Banday, R. B. Barreiro, N. Bartolo, et al., *Planck 2018 results. vi. cosmological parameters* (2018), 1807.06209.

- [14] E. Di Valentino, *Nature Astronomy* **1**, 569 (2017), 1709.04046.
- [15] A. G. Riess, S. Casertano, W. Yuan, L. M. Macri, and D. Scolnic, *Astrophys. J.* **876**, 85 (2019), 1903.07603.
- [16] M. Kilbinger, L. Fu, C. Heymans, F. Simpson, J. Benjamin, T. Erben, J. Harnois-Déraps, H. Hoekstra, H. Hildebrandt, T. D. Kitching, et al., *Mon. Not. R. Astron. Soc.* **430**, 2200 (2013), 1212.3338.
- [17] F. Köhlinger, M. Viola, B. Joachimi, H. Hoekstra, E. van Uitert, H. Hildebrandt, A. Choi, T. Erben, C. Heymans, S. Joudaki, et al., *Mon. Not. R. Astron. Soc.* **471**, 4412 (2017), 1706.02892.
- [18] H. Hildebrandt, M. Viola, C. Heymans, S. Joudaki, K. Kuijken, C. Blake, T. Erben, B. Joachimi, D. Klaes, L. Miller, et al., *Mon. Not. R. Astron. Soc.* **465**, 1454 (2017), 1606.05338.
- [19] S. Joudaki, C. Blake, A. Johnson, A. Amon, M. Asgari, A. Choi, T. Erben, K. Glazebrook, J. Harnois-Déraps, C. Heymans, et al., *Mon. Not. R. Astron. Soc.* **474**, 4894 (2018), 1707.06627.
- [20] L. Guzzo, M. Pierleoni, B. Meneux, E. Branchini, O. Le Fèvre, C. Marinoni, B. Garilli, J. Blaizot, G. De Lucia, A. Pollo, et al., *Nature (London)* **451**, 541 (2008), 0802.1944.
- [21] V. Salvatelli, N. Said, M. Bruni, A. Melchiorri, and D. Wands, *Physical Review Letters* **113**, 181301 (2014), 1406.7297.
- [22] W. Yang and L. Xu, *Phys. Rev. D* **90**, 083532 (2014), 1409.5533.
- [23] W. Yang and L. Xu, *Phys. Rev. D* **89**, 083517 (2014), 1401.1286.
- [24] R. C. Nunes, S. Pan, and E. N. Saridakis, *Phys. Rev. D* **94**, 023508 (2016), 1605.01712.
- [25] C. van de Bruck, J. Mifsud, and J. Morrice, *Phys. Rev. D* **95**, 043513 (2017), 1609.09855.
- [26] W. Yang, H. Li, Y. Wu, and J. Lu, *JCAP*. **10**, 007 (2016), 1608.07039.
- [27] C. van de Bruck and C. C. Thomas, *Phys. Rev. D* **100**, 023515 (2019), 1904.07082.
- [28] W. Yang, S. Pan, and A. Paliathanasis, *Mon. Not. R. Astron. Soc.* **482**, 1007 (2019), 1804.08558.
- [29] M. Martinelli, N. B. Hogg, S. Peirone, M. Bruni, and D. Wands, *Mon. Not. R. Astron. Soc.* **488**, 3423 (2019), 1902.10694.
- [30] S. Pan, W. Yang, and A. Paliathanasis, *Monthly Notices of the Royal Astronomical Society* **493**, 3114 (2020), ISSN 0035-8711, <https://academic.oup.com/mnras/article-pdf/493/3/3114/32890756/staa213.pdf>, URL <https://doi.org/10.1093/mnras/staa213>.
- [31] X.-J. Bi, B. Feng, H. Li, and X. Zhang, *Phys. Rev. D* **72**, 123523 (2005), hep-ph/0412002.
- [32] R.-Y. Guo, J.-F. Zhang, and X. Zhang, *Chinese Physics C* **42**, 095103 (2018), 1803.06910.
- [33] C. van de Bruck and J. Mifsud, *Physical Review D* **97** (2018), ISSN 2470-0029, URL <http://dx.doi.org/10.1103/PhysRevD.97.023506>.
- [34] S. Vagnozzi, S. Dhawan, M. Gerbino, K. Freese, A. Goobar, and O. Mena, *Phys. Rev. D* **98**, 083501 (2018), 1801.08553.
- [35] S. Betts, W. R. Blanchard, R. H. Carnevale, C. Chang, C. Chen, S. Chidzik, L. Ciebiera, P. Cloessner, A. Cocco, A. Cohen, et al., *arXiv e-prints arXiv:1307.4738* (2013), 1307.4738.
- [36] J. Lesgourgues and S. Pastor, 307 (2006), astro-ph/0603494.
- [37] L. Feng, H.-L. Li, J.-F. Zhang, and X. Zhang, *Science China Physics, Mechanics, and Astronomy* **63**, 220401 (2020), 1903.08848.
- [38] M. B. Gavela, D. Hernández, L. Lopez Honorez, O. Mena, and S. Rigolin, *JCAP*. **2009**, 034 (2009), 0901.1611.
- [39] M. Quartin, M. O. Calvão, S. E. Jorás, R. R. R. Reis, and I. Waga, *JCAP*. **2008**, 007 (2008), 0802.0546.
- [40] C. G. Böhrer, G. Caldera-Cabral, R. Lazkoz, and R. Maartens, *Phys. Rev. D* **78**, 023505 (2008), 0801.1565.
- [41] C. Böhrer, G. Caldera-Cabral, R. Lazkoz, and R. Maartens, in *American Institute of Physics Conference Series*, edited by K. E. Kunze, M. Mars, and M. A. Vázquez-Mozo (2009), vol. 1122 of *American Institute of Physics Conference Series*, pp. 197–200.
- [42] W. Zimdahl and D. Pavón, *Classical and Quantum Gravity* **24**, 5461 (2007), astro-ph/0606555.
- [43] R. R. Bachega, A. A. Costa, E. Abdalla, and K. Fornazier, *Journal of Cosmology and Astroparticle Physics* **2020**, 021–021 (2020), ISSN 1475-7516, URL <http://dx.doi.org/10.1088/1475-7516/2020/05/021>.
- [44] Y.-H. Li, J.-F. Zhang, and X. Zhang, *Phys. Rev. D* **90**, 063005 (2014), 1404.5220.
- [45] Y.-H. Li, J.-F. Zhang, and X. Zhang, *Phys. Rev. D* **90**, 123007 (2014), 1409.7205.
- [46] R.-Y. Guo, Y.-H. Li, J.-F. Zhang, and X. Zhang, *JCAP*. **2017**, 040 (2017), 1702.04189.
- [47] X. Zhang, *Science China Physics, Mechanics, and Astronomy* **60**, 50431 (2017), 1702.04564.
- [48] J.-P. Dai and J.-Q. Xia, *Astrophys. J.* **876**, 125 (2019), 1904.04149.
- [49] W. Yang, S. Pan, E. Di Valentino, R. C. Nunes, S. Vagnozzi, and D. F. Mota, *JCAP*. **2018**, 019 (2018), 1805.08252.
- [50] C.-P. Ma and E. Bertschinger, *Astrophys. J.* **455**, 7 (1995), astro-ph/9506072.
- [51] B. M. Jackson, A. Taylor, and A. Berera, *Phys. Rev. D* **79**, 043526 (2009), 0901.3272.
- [52] M. B. Gavela, L. Lopez Honorez, O. Mena, and S. Rigolin, *JCAP*. **2010**, 044 (2010), 1005.0295.
- [53] V. Salvatelli, A. Marchini, L. Lopez-Honorez, and O. Mena, *Phys. Rev. D* **88**, 023531 (2013), 1304.7119.
- [54] L. Feng, J.-F. Zhang, and X. Zhang, *Physics of the Dark Universe* **23**, 100261 (2019), 1712.03148.
- [55] G. Ballesteros and J. Lesgourgues, *JCAP*. **2010**, 014 (2010), 1004.5509.
- [56] J.-Q. Xia, Y.-F. Cai, T.-T. Qiu, G.-B. Zhao, and X. Zhang, *International Journal of Modern Physics D* **17**, 1229 (2008), astro-ph/0703202.
- [57] R. J. F. Marcondes, R. C. G. Landim, A. A. Costa, B. Wang, and E. Abdalla, *JCAP*. **2016**, 009 (2016), 1605.05264.
- [58] J. B. Jiménez, L. Heisenberg, T. Koivisto, and S. Pekar, *Phys. Rev. D* **101**, 103507 (2020), 1906.10027.
- [59] B. J. Barros, T. Barreiro, T. Koivisto, and N. J. Nunes, *Physics of the Dark Universe* **30**, 100616 (2020), 2004.07867.
- [60] E. V. Linder and R. N. Cahn, *Astroparticle Physics* **28**, 481 (2007), astro-ph/0701317.
- [61] M. J. Hudson and S. J. Turnbull, *The Astrophysical Journal* **751**, L30 (2012), ISSN 2041-8213, URL <http://dx.doi.org/10.1088/0007-1385/751/L30/000>.

doi.org/10.1088/2041-8205/751/2/L30.

- [62] B. Sagredo, S. Nesseris, and D. Sapone, *Phys. Rev. D* **98**, 083543 (2018), 1806.10822.
- [63] D. M. Scolnic, D. O. Jones, A. Rest, Y. C. Pan, R. Chornock, R. J. Foley, M. E. Huber, R. Kessler, G. Narayan, A. G. Riess, et al., *Astrophys. J.* **859**, 101 (2018), 1710.00845.
- [64] F. Beutler, C. Blake, M. Colless, D. H. Jones, L. Staveley-Smith, L. Campbell, Q. Parker, W. Saunders, and F. Watson, *Mon. Not. R. Astron. Soc.* **416**, 3017 (2011), 1106.3366.
- [65] A. J. Ross, L. Samushia, C. Howlett, W. J. Percival, A. Burden, and M. Manera, *Mon. Not. R. Astron. Soc.* **449**, 835 (2015), 1409.3242.
- [66] L. Anderson, É. Aubourg, S. Bailey, F. Beutler, V. Bhardwaj, M. Blanton, A. S. Bolton, J. Brinkmann, J. R. Brownstein, A. Burden, et al., *Mon. Not. R. Astron. Soc.* **441**, 24 (2014), 1312.4877.
- [67] N. Padmanabhan, X. Xu, D. J. Eisenstein, R. Scalzo, A. J. Cuesta, K. T. Mehta, and E. Kazin, *Mon. Not. R. Astron. Soc.* **427**, 2132 (2012), 1202.0090.
- [68] C. Blake, S. Brough, M. Colless, C. Contreras, W. Couch, S. Croom, D. Croton, T. M. Davis, M. J. Drinkwater, K. Forster, et al., *Mon. Not. R. Astron. Soc.* **425**, 405 (2012), 1204.3674.
- [69] T. Delubac, J. E. Bautista, N. G. Busca, J. Rich, D. Kirkby, S. Bailey, A. Font-Ribera, A. Slosar, K.-G. Lee, M. M. Pieri, et al., *Astron. Astrophys.* **574**, A59 (2015), 1404.1801.
- [70] S. W. Hell, S. J. Sahl, M. Bates, X. Zhuang, R. Heintzmann, M. J. Booth, J. Bewersdorf, G. Shtengel, H. Hess, P. Tinnefeld, et al., *Journal of Physics D Applied Physics* **48**, 443001 (2015), 1711.04999.
- [71] S. Alam, M. Ata, S. Bailey, F. Beutler, D. Bizyaev, J. A. Blazek, A. S. Bolton, J. R. Brownstein, A. Burden, C.-H. Chuang, et al., *Mon. Not. R. Astron. Soc.* **470**, 2617 (2017), 1607.03155.
- [72] H. du Mas des Bourboux, J.-M. Le Goff, M. Blomqvist, N. G. Busca, J. Guy, J. Rich, C. Yèche, J. E. Bautista, É. Burtin, and K. S. Dawson, *Astron. Astrophys.* **608**, A130 (2017), 1708.02225.
- [73] Planck Collaboration, N. Aghanim, Y. Akrami, M. Ashdown, J. Aumont, C. Baccigalupi, M. Ballardini, A. J. Banday, R. B. Barreiro, N. Bartolo, et al., *Astron. Astrophys.* **641**, A5 (2020), 1907.12875.
- [74] W. Hu and N. Sugiyama, *Astrophys. J.* **471**, 542 (1996), astro-ph/9510117.
- [75] S. Cao, N. Liang, and Z.-H. Zhu, *Monthly Notices of the Royal Astronomical Society* **416**, 1099–1104 (2011), ISSN 0035-8711, URL <http://dx.doi.org/10.1111/j.1365-2966.2011.19105.x>.
- [76] R. Lazkoz and E. Majerotto, *Journal of Cosmology and Astroparticle Physics* **2007**, 015–015 (2007), ISSN 1475-7516, URL <http://dx.doi.org/10.1088/1475-7516/2007/07/015>.
- [77] M. Moresco, L. Pozzetti, A. Cimatti, R. Jimenez, C. Maraston, L. Verde, D. Thomas, A. Citro, R. Tojeiro, and D. Wilkinson, *Journal of Cosmology and Astroparticle Physics* **2016**, 014–014 (2016), ISSN 1475-7516, URL <http://dx.doi.org/10.1088/1475-7516/2016/05/014>.
- [78] R. Jimenez and A. Loeb, *Astrophys. J.* **573**, 37 (2002), astro-ph/0106145.
- [79] D. Blas, J. Lesgourgues, and T. Tram, *JCAP* **7**, 034 (2011), 1104.2933.
- [80] B. Audren, J. Lesgourgues, K. Benabed, and S. Prunet, *JCAP* **1302**, 001 (2013), 1210.7183.
- [81] T. Brinckmann and J. Lesgourgues (2018), 1804.07261.
- [82] H. G. Katzgraber, *Introduction to monte carlo methods* (2011), 0905.1629.
- [83] E. Di Valentino and S. Bridle, *Symmetry* **10** (2018), ISSN 2073-8994, URL <https://www.mdpi.com/2073-8994/10/11/585>.
- [84] S. F. King, *Contemporary Physics* **48**, 195 (2007), <https://doi.org/10.1080/00107510701770539>, URL <https://doi.org/10.1080/00107510701770539>.
- [85] K. Yoshikawa, S. Tanaka, N. Yoshida, and S. Saito, arXiv e-prints arXiv:2010.00248 (2020), 2010.00248.
- [86] P. Coloma, M. C. Gonzalez-Garcia, and M. Maltoni, arXiv e-prints arXiv:2009.14220 (2020), 2009.14220.